Use of unstressed strands for connections of precast concrete members

Xiao Liang and Sri Sritharan

- This paper investigates the use of unstressed strands as connection reinforcement for precast concrete members through both experimental and analytical programs. The primary focus of the study was to establish positive moment connections using unstressed strands between precast concrete girders and a cap beam for seismic applications.

- An experimental program was designed to investigate the fundamental load-transfer characteristics of unstressed strands. A total of 20 pullout tests were conducted with varying parameters, including strand diameter, anchorage detail, embedment length, and loading type.

- An analytical program examined the bond stress of unstressed strands, and design guidelines for using unstressed strands to connect precast concrete members are presented.

PCI Journal (ISSN 0887-9672) V. 66, No. 3, May–June 2021.

PCI Journal is published bimonthly by the Precast/Prestressed Concrete Institute, 8770 W. Bryn Mawr Ave., Suite 1150, Chicago, IL 60631.

Prefabricated construction techniques using precast concrete members are known to provide better quality control and a more efficient construction process than traditional construction techniques involving cast-in-place concrete. The precast concrete members are generally fabricated off-site and connected on-site to form an integral structural system. Therefore, effective and feasible field connections are essential to ensure satisfactory performance of structures designed with precast concrete components.

In current industry practice, dry and wet connections are two commonly used techniques to connect precast concrete members and develop adequate capacity within the connection region. A wet connection is defined as reinforcement in the connection region that is spliced with mechanical couplers, welds, or lap splices, and filled with grout or cast-in-place concrete. A dry connection is any other type of connection.[1]

Although not used frequently, extending prestressing strands from the ends of precast concrete members into the connection region provides a cost-effective and easily implementable wet connection for several reasons. First, strands are flexible, and thus they can be easily routed and positioned within the connection. Second, strands present high tensile strength, therefore requiring significantly fewer of them for the same connection capacity compared with mild reinforcing bars. Third, strands used for pretensioning the precast concrete members do not have to be cut off after full development of concrete strength; they can be extended from the member end and serve as splice reinforcement instead of embedding additional reinforcing bars or couplers, thereby eliminating reinforcement congestion within the precast concrete members.

Although extending prestressing strands into connection regions offers several benefits, its response has not been studied adequately, as evidenced by the lack of available design guidelines. The extended strands in the connection region are unstressed after the prestressing force is transferred within the precast concrete members. Therefore, the bond between prestressing strands and the surrounding concrete due to wedge action, also known as the Hoyer effect, does not contribute to the performance of unstressed strands in the connection region. This means the anchorage length must be longer for unstressed strands than for prestressing strands that benefit from the Hoyer effect. The American Association of State Highway and Transportation Officials' *AASHTO LRFD Bridge Design Specifications*[2] allow the use of unstressed strands in design; however, the maximum allowable stress in these strands is recommended to be limited to $0.80f_{py}$ at service limit state after losses, where f_{py} is the yield strength of prestressing steel. This limit is recommended partly because prestressing steel does not have a well-defined yield plateau. It also presents significantly lower ductility than mild reinforcing bars. Furthermore, the AASHTO LRFD specifications require the structural performance of unstressed strands to be experimentally validated to satisfy the design requirements.

Given the aforementioned concerns with regard to the use of unstressed strands in precast concrete member connections, this paper investigates the use of unstressed strands as the connection reinforcement in conjunction with precast concrete members through a combination of experimental and analytical studies in three parts. Unstressed strands that either extended from the ends of precast concrete members or were placed within grouted ducts were considered in this investigation. First, an experimental program based on pullout tests was designed to investigate the fundamental load-transfer characteristics of unstressed strands. Twenty pullout tests were conducted with the strand diameter, anchorage detail, embedment length, and loading type as the main investigated variables. An analytical program was then developed to examine the bond stress of unstressed strands. Finally, design guidelines for using unstressed strands to connect precast concrete members are presented. Although the focus of the study presented herein is to establish positive moment connections using unstressed strands between precast concrete girders and a cap beam for seismic applications, the results can be extended to other scenarios involving precast concrete members and wet connections.

Previous research and limitations

To examine the use of unstressed, bonded strands as connection reinforcement for precast concrete members, especially for precast concrete bridge girder applications, previous researchers have studied the bond characteristics of unstressed strands through pullout tests and the performance of connection details through large-scale system tests.

In the mid-1970s, Salmons and McCrate[3] performed pullout tests to examine the bond characteristics of unstressed strands with three different configurations: straight unfrayed, straight frayed, and bent unfrayed. The test strands were embedded in concrete with different embedment lengths. The concrete compressive strength was in a range of 3750 to 6900 psi (25.86 to 47.57 MPa). The relationships between the strand stress and slip at the loaded end were established, and the relationships between the embedment length and the strand stress at the general slip were formulated based on a least squares fit of the data for the three strand configurations. The general slip was defined as the point at which the slip at the unloaded end of a strand was sufficient to produce a readable measurement. It was found that the bent unfrayed strands provided the highest strength and stiffness, followed by the straight unfrayed strands. The straight frayed strands showed the lowest strength and stiffness. In addition, concrete compressive strength and strand diameter were not found to have significant effects on the bond characteristics of unstressed strands. Because the scope of this study was not to determine the ultimate capacity of unstressed strands, the tests were terminated when the general slip condition occurred. Therefore, the load-displacement response beyond the general slip condition up to the ultimate strength of strands was not developed.[3]

Noppakunwijai et al.[4] conducted pullout tests of unstressed bent strands. The test setup replicated a positive connection region between two adjacent precast concrete girders used in nonseismic regions. They evaluated the pullout capacity of 0.5 and 0.6 in. (12.7 and 15.2 mm) diameter, Grade 270 (1860 MPa), low-relaxation, unstressed bent strands with different embedment lengths in concrete with a specified compressive strength of 4000 psi (28 MPa). The embedment length was defined as the sum of the horizontal embedment length (distance from the end face of the precast concrete I-girder to the centerline of the vertical leg of the extended strand) and vertical embedment length (vertical portion of the extended bent strand in the diaphragm). It was found that the pullout capacity increased with increasing embedment length. For a fixed horizontal embedment length (6 in. [152.4 mm]) corresponding to the common diaphragm dimensions, a design equation was developed for the vertical embedment length to achieve the maximum strand stress, which was conservatively taken as 80% of the specified tensile strength of strands ($0.8f_{pu}$). Based on this design equation, minimum total embedment lengths of 30 and 36 in. (762 and 914 mm) were recommended for 0.5 and 0.6 in. diameter strands, respectively.

Following the pullout test findings reported by Salmons and McCrate,[3] Miller et al.[5] systematically investigated the performance of six positive moment connection details to resist concrete cracking caused by positive moment, two of which used extended unstressed strands. The experimental results showed that the extended strand connections developed adequate strength to resist the cracking moment. To further validate the connection performance, they tested a full-scale 100 ft (30.5 m) long, continuous-for-live-load precast concrete girder using an extended strand connection with a composite concrete deck slab cast on top. Although several U.S. states use the bent-strand type of connection to provide positive moment at the diaphragm, the AASHTO LRFD specifications do not provide specific requirements or guidelines for the strand anchorage. The large-scale experimental testing confirmed that the extended bent-strand type of connection provided sufficient positive moment capacity;[5] however, the test was terminated before it experienced any failures because this system was also intended to be used to test the negative moment capacity.

The connection details studied by Miller et al.[5] were designed to resist positive moment caused primarily by time-dependent effects such as creep, shrinkage, and temperature. However, high-quality, efficient bridges with precast concrete components are also preferred in seismic regions, where the positive moment demand of the connections is significantly greater than the cracking moment caused by time-dependent effects. The inverted-tee bent cap–to–precast concrete I-girder connection has been used widely in California. The current California Department of Transportation (Caltrans) Seismic *Design Criteria*[6] assumes this connection degrades to a pinned connection during a seismic event, which means that precast concrete girder bridges are not cost-effective in seismic regions.[7] Consequently, Vander Werff et al.[8] studied the seismic response and overall moment resistance of this inverted-tee connection concept and found that when subjected to seismic loading, it developed sufficient moment resistance to ensure formation of plastic hinges at the column top.

Figure 1 shows two proposed design concepts for cost-effective and easily implementable connections in seismic regions. In the first, unstressed strands are placed and grouted inside tubes continuously along the partial or full length of each girder on either side and through the cap beam. In the second, unstressed strands are extended from the end of precast concrete girders and anchored within the cap beam with a 90-degree bend or end plates. To complement these two connection design concepts, a pullout test program was designed to understand the load-transfer characteristics of unstressed strands that are used as connection reinforcement.

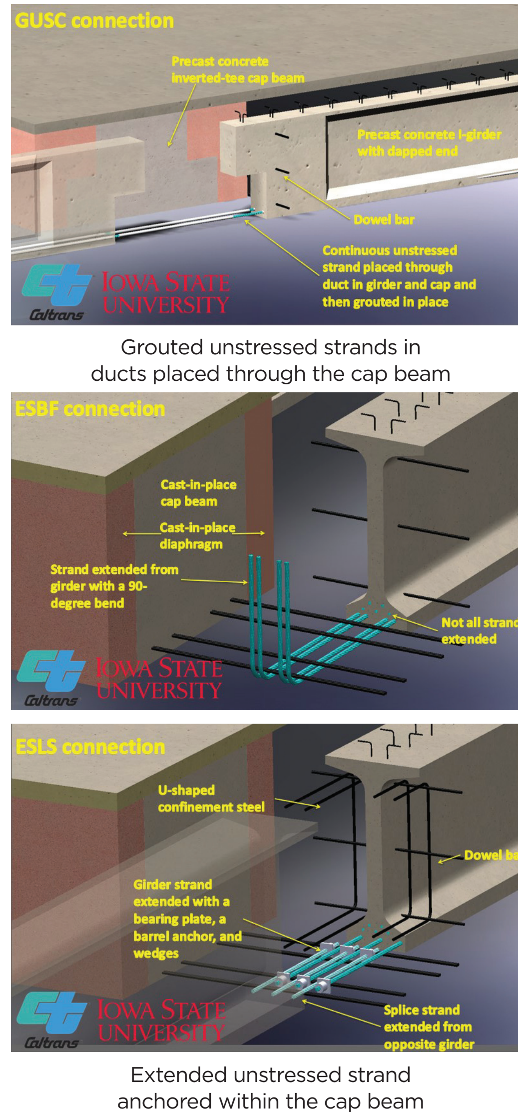

Figure 1. Positive moment connection details proposed for seismic design. Source: Reproduced from Vander Werff et al. (2015). Note: Caltrans = California Department of Transportation; ESBF = extended strand bent with free end; ESLS = extended strand with a lap splice: GUSC = grouted unstressed strand connection.

Experimental program

A total of 20 strands were embedded in three large-scale reinforced concrete blocks that represented bridge cap beams and diaphragms. The main variables investigated were strand diameter, anchorage detail at the strand end, embedment length, and loading type. The strands were required to develop their ultimate strength due to their use in seismic design. With the results of the experimental study, the understanding of bond characteristics for unstressed strands has been significantly improved and a series of design recommendations has been made with regard to the use of unstressed strands as the connection reinforcement for precast concrete members.

Two sets of pullout tests were designed to study the load-transfer characteristics of unstressed strands. The first set was used for grouted unstressed strands, which simulated connections with unstressed strands placed inside corrugated ducts along partial or full girder lengths and through the cap beam. The second set was designed for extended, unstressed strands anchored in concrete, which simulated connections with unstressed strands extended from the end of a precast concrete bridge girder and anchored within the cap beam.

The first set of tests used a reinforced concrete block that was designed to replicate the bottom portion (**Fig. 2**) of a 50%

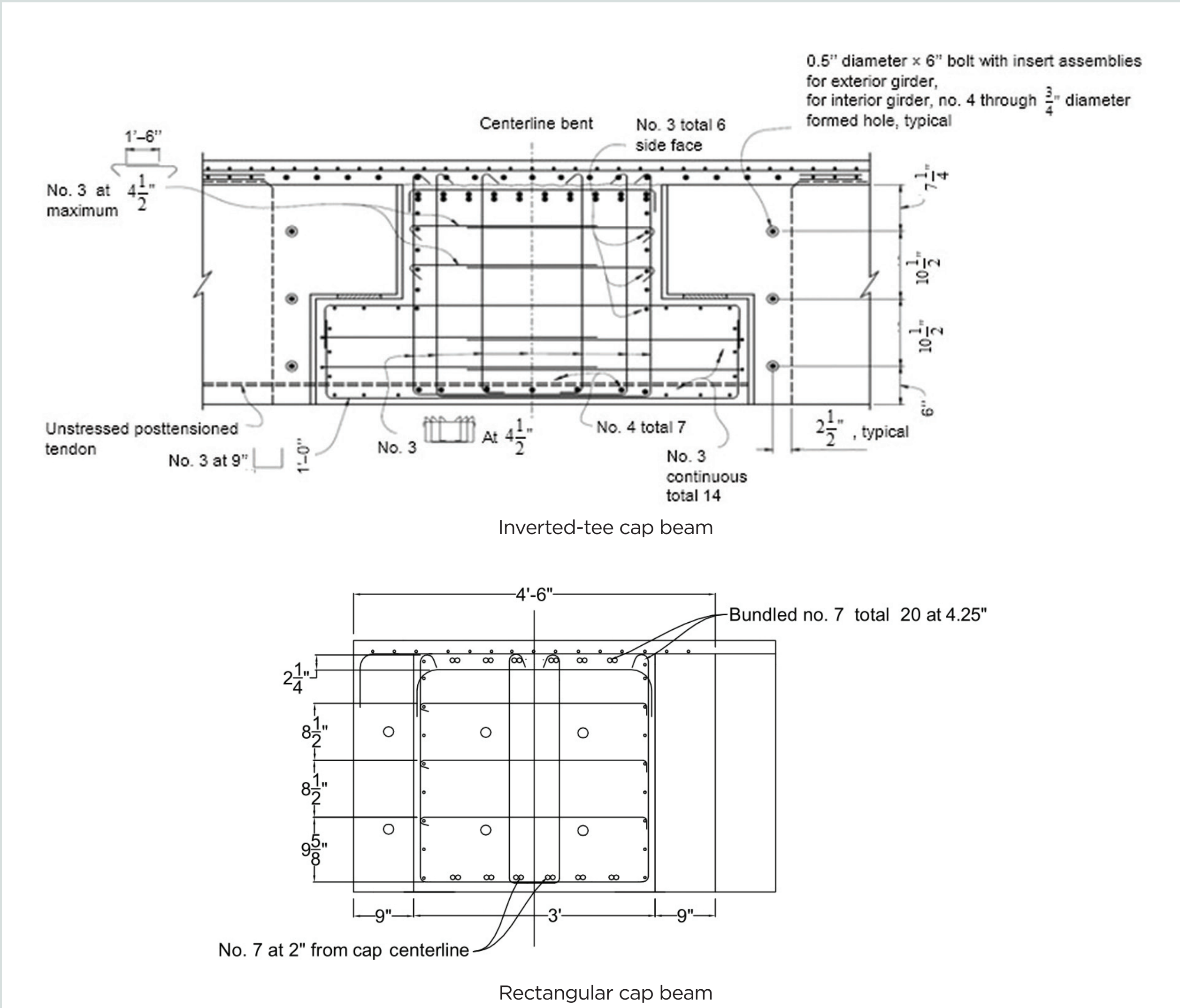

Figure 2. Cap beam used in test specimens. Source: Reproduced from Vander Werff et al. (2015). Note: no. 3 = 10M; no. 4 = 13M; no. 7 = 22M; 1" = 1 in. = 25.4 mm; 1' = 1 ft = 0.305 m.

scale typical inverted-tee cap beam that has been widely used in California. The second set used two reinforced concrete blocks that were designed to replicate a 40% scale rectangular cap beam suitable to support bulb-tee girders (Figure 2).

For the first set, the pullout tests were conducted on 0.375 in. (9.5 mm) diameter strands with four test variables: initial stress, tendon curvature, loading type (monotonic or cyclic), and number of strands in a duct (one or two). When a girder is installed in line with a column, the ducts are typically placed around the column to simplify construction. The strand with curved tendon was used to simulate this strand configuration.

For the second set, the pullout tests were performed using three strand sizes (0.375, 0.5, and 0.6 in. [9.5, 12.7, and 15.2 mm] diameter) and two loading types (monotonic and cyclic). These strands were embedded in two reinforced concrete blocks with four different anchorage details at the strand ends: straight with free end, 90-degree bend with free end, straight with bond head, and straight with end plate. Strands with straight and free end anchorages were embedded along the entire length of the reinforced concrete block. Strands with 90-degree bends and free ends were designed with a 6 in. pre-bent length for 0.375 in. diameter strands, which gave a total embedment length of 42 in. (1067 mm). This pre-bent length was selected to be consistent with the study by Salmons and McCrate.[3] An increased tail length of 8 in. (203 mm) was used for 0.5 in. diameter strands, which provided a total embedment length of 56 in. (1422 mm). The strand wires are plastically deformed at the end by the strand manufacturer for the bond head, and this anchorage was expected to be provided by the bond between the deformed strand wires and surrounding concrete. For the straight strands anchored with end plates, the bearing plates were designed to be 4 × 4 × 5/8 in. (101.6 × 101.6 × 15.9 mm) thick. The strand chuck was attached to the bearing plate using tack welding. It was expected that using bond-head and end-plate anchorages at the strand end would reduce the required embedment lengths. Therefore, strands with bond-head and end-plate anchorages were tested with significantly shorter embedment lengths, which ranged from 18 to 30 in. (457.2 to 762 mm).

Figure 3 shows the pullout test setup. The reinforced concrete block was supported by two I-shaped steel beams at each end and was post-tensioned to the strong floor through high-strength threaded rods. A movable steel frame was used to test one strand at a time to avoid affecting the behavior of the test strand. After completing the first set of pullout tests, a portable setup using a steel chair was designed for the second set. Previous studies[3-4] have shown that the compression force applied by a steel chair to a concrete block does not have a significant effect on the behavior of strand pullout, and this setup was easy to move among the different tests. For both test sets, the strands were pulled out of the concrete block using a hydraulic ram.

The minimum spacing between two strands was 18 in. (457.2 mm) to avoid potential development of splitting cracks between strands. The strands were loaded until they experienced pullout or rupture failure.

Table 1 provides a summary of all pullout tests performed in this study. Each strand was assigned an identification name according to the investigated parameters. The first letter, C or G, indicates whether the strand was embedded in concrete or grouted ducts. If the strand was embedded in concrete, the letter D and the number immediately following it represent the strand diameter, with 3, 5, or 6 corresponding to a strand diameter of 0.375, 0.5, or 0.6 in. (9.5, 12.7, or 15.2 mm), respectively. After the strand diameter is the anchorage type, with S, 90Deg, Bulb, or Plate representing straight with free end, 90-degree bend with free end, straight with bond-head anchorage, or straight with end-plate anchorage, respectively. The number immediately following the anchorage type represents the embedment length. In addition, Cyclic or M, indicates whether the strand was subjected to cyclic or monotonic loading, respectively. For example, C-D6-Plate18-M corresponds to a 0.6 in. diameter strand embedded in concrete with an end-plate anchorage, which had an embedment length of 18 in. (457.2 mm) and was subjected to monotonic loading. A similar naming convention was applied to the strands embedded in grouted ducts. Parameters specifically tested for strands embedded in grouted ducts are given in parentheses following the loading type, with 1, 2, or I representing one strand per duct, two strands per duct, or strand with initial stress, respectively.

Test procedure

Instrumentation

The load and displacement at the loading end of a strand were measured during each pullout test. The load was measured using a load cell and the loaded-end displacement was measured using direct current displacement transducers (DCDTs). For the straight strands anchored along the entire length of the

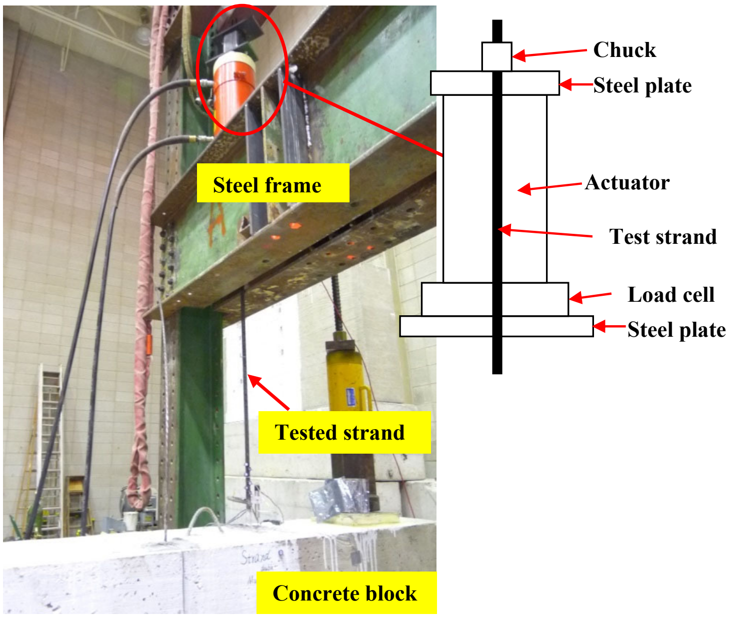

Figure 3. Test setup.

Table 1. Experimental test matrix

	Strand diameter, in.	Initial stress, ksi	Anchorage length, in.	Loading history	Anchorage type
Strands embedded in concrete	0.375	0	54 (straight)	Monotonic	No
	0.375	0	54 (straight)	Cyclic	No
	0.6	0	54 (straight)	Monotonic	No
	0.375	0	36 + 6 pre-bent length	Monotonic	90-degree bend
	0.375	0	36 + 6 pre-bent length	Cyclic	90-degree bend
	0.5	0	48 + 8 pre-bent length	Monotonic	90-degree bend
	0.5	0	48 + 8 pre-bent length	Cyclic	90-degree bend
	0.6	0	1	Monotonic	Bond head
	0.6	0	1	Cyclic	Bond head
	0.6	0	18	Monotonic	Bond head
	0.6	0	18	Cyclic	Bond head
	0.6	0	24	Cyclic	Bond head
	0.6	0	18	Monotonic	End plate
	0.6	0	24	Cyclic	End plate
	0.6	0	30	Cyclic	End plate
Strands embedded in ducts filled with grout	0.375	0	48 (straight)	Monotonic	No
	0.375	0	48 (straight)	Monotonic	No
	0.375	25	48 (straight)	Monotonic	No
	0.375	0	60 (curved)	Monotonic	Curved
	0.375	0	48 (straight)	Cyclic	No

Note: 1 in. = 25.4 mm; 1 ksi = 6.895 MPa.

concrete block, DCDTs were used on both sides of the block to measure the displacement at the loading and free ends of the strands. For the strand anchored inside the concrete block, a DCDT was installed at the loading end only. A three-dimensional motion-capture system was used to measure the displacement at the loading end for more detailed measurements, and the displacement of strands at target points was measured using smart markers. Four markers were placed on the strand beyond the bonded region, one was placed at the side surface of the concrete block to monitor its movement, and another was attached to the DCDT at the loading end to calibrate the DCDT's readings. Strains were also measured for each test strand; one strain gauge was placed at the loading end and several were placed along the embedment length to monitor the load transfer along the bonded length of the strands. The data collection frequency of the data acquisition system was set to 50 Hz. **Figure 4** shows the instrumentation details for the tested strands. It was assumed that the strain was constant over the length between the displacement measurement location and the concrete block surface at the loading end. Therefore, the loaded-end displacement was calculated from the measured displacements and strains by subtracting the extension of the strand between the location of the displacement measurement and the surface of the concrete block. Figure 4 presents the strain gauge locations along the embedment length. For the straight strands anchored with a 90-degree bend, one strain gauge was placed at the bend location and two strain gauges were placed at equal distances from this strain gauge at the pre-bent and straight bonded region, respectively. For the strand grouted in duct and tested with an initial stress, the strain gauges were placed 0.25 in. (6.4 mm) below the target locations of the strands without an initial stress to account for the effect of initial stress and the strains were measured at the same locations. At each location, two strain gauges were placed on opposite sides of the strand to increase the measurement reliability.

Loading protocol

For the monotonic experiments, the strand was subjected to increasing monotonic tension forces under force control until it experienced yielding, after which a displacement control was used until the end of the test. The load was applied in four steps in the elastic range and a number of displacement

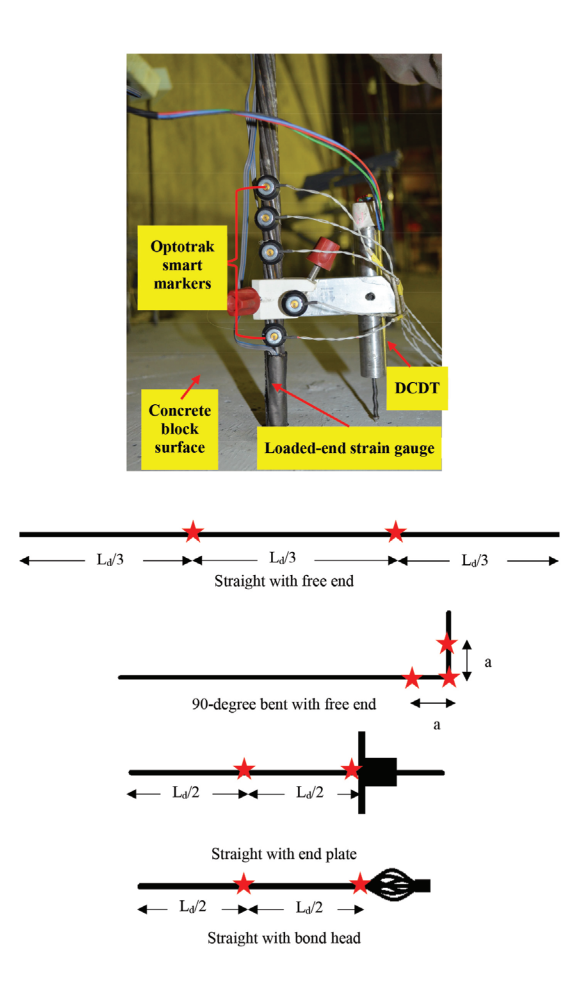

Figure 4. Instrumentation details. Note: a = pre-bent length; DCDT = direct current displacement transducer; L_d = embedment length.

steps were used after the strand reached the yield strain, with the displacement adjusted at each load step. For the cyclic tests, the strand was subjected to a half-cycle at each specified force level in the elastic range and then subjected to three half-cycles at each target loaded-end displacement until it experienced rupture or pullout failure.

Experimental results

Table 2 summarizes the pullout test results, which include the strand stress at the first free-end displacement (that is, the strand stress corresponding to the first readable measurement at the free end of the strand), strand stress when the first wire fractured, maximum strand stress, peak load, failure mode, and number of wires fractured at the end of each test. The following sections present the experimental results for strands embedded in grouted ducts and for strands bonded in concrete. The behaviors of the strands are then compared and discussed, as are the anchorage capacities of the four anchorage details considered in this research.

Strands embedded in grouted ducts

General behavior and failure modes Among the five strands embedded in grouted ducts, two of them experienced pullout failure: the strand with initial stress and the single strand in a duct subjected to monotonic loading. The remaining three strands experienced rupture failure. Although the single strand in a duct subjected to cyclic loading experienced rupture failure, it showed twice the ultimate loaded-end displacement of the other two with the rupture failure (0.8 in. [20.3 mm] compared with 0.4 in. [10.2 mm]). For all five strands embedded in grouted ducts, the stress at the first wire fracture was around 230 ksi (1586 MPa) ($0.85f_{pu}$) and the peak load was approximately 20 kip (89 kN).

Comparison of strand stress and loaded-end displacement **Figure 5** shows the relationship between the strand stress and loaded-end displacement for all strands anchored in grouted ducts. The single strand in a duct reached its capacity when subjected to cyclic loading, which was not the case for the monotonically loaded strand. The cause of the poor behavior of the latter strand was suspected to be insufficient grouting that failed to fully bond the strand. The failure of the strand subjected to cyclic loading was characterized by the strand rupture, but it experienced significant loaded-end displacement. During the test, this strand started to experience free-end displacement when the stress reached 191 ksi (1317 MPa) and had a free-end displacement of 0.4 in. (10.2 mm) at the end of the test. This ultimate free-end displacement contributed approximately 50% of the total displacement measured at the loading end, which explains the significant displacement measured at the loading end for cyclic loading. This observation indicates that strain penetration occurred along the entire embedment length of 48 in. (1219 mm) ($128d_s$ where d_s is the strand diameter) after the stress reached 191 ksi, resulting in significant free-end displacement. Two strands placed in a duct also behaved favor-

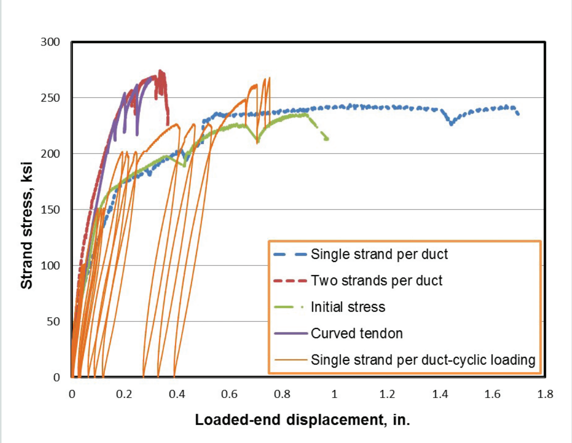

Figure 5. Strand stress–displacement response comparisons of strands anchored in grouted ducts. Note: 1 in. = 25.4 mm; 1 ksi = 6.895 MPa.

Table 2. Experimental test results summary

	Specimen	Strand stress at first free-end slip, ksi	Strand stress at first wire fractured, ksi	Maximum strand stress, ksi	Peak load, kip	Failure mode	Fractured wires	Anchorage type
Strands embedded in concrete	C-D3-S54-M	No free-end slip was observed	245	270	20.8	Strand rupture	5	Straight
	C-D3-S54-Cyclic	140 (first cycle to 12 kip) compared with 161.54 ksi (Salmons and McCrate)	No wire was fractured	234	20	Bond failure	0	
	C-D6-S54-M	230	No wire was fractured	230	50	Bond failure	0	
	C-D3-90Deg42-M	n/a	260	260	22	Strand rupture	4	90-degree bent
	C-D3-90Deg42-Cyclic	n/a	257	257	22	Strand rupture	4	
	C-D5-90Deg56-M	n/a	279	281	43	Strand rupture	7 (1 + 6 at the same time)	
	C-D5-90Deg56-Cyclic	n/a	280	281	43	Strand rupture	7 (at the same time)	
	C-D6-Bulb0-M	n/a	No wire was fractured	212.8	46	Bond failure	0	Bond head
	C-D6-Bulb0-Cyclic	n/a	No wire was fractured	240.7	52	Bond failure	0	
	C-D6-Bulb18-M	n/a	270	310	60	Strand rupture, bond failure	2	
	C-D6-Bulb18-Cyclic	n/a	No wire was fractured	180	39	Bond failure	0	
	C-D6-Bulb22-Cyclic	n/a	No wire was fractured	250	54	Bond failure	0	
	C-D6-Plate18-M	n/a	271	274.5	59.5	Strand rupture	4	End plate
	C-D6-Plate24-Cyclic	n/a	278	281	61	Strand rupture	7 (at the same time)	
	C-D6-Plate30-Cyclic	n/a	279	279	60.6	Strand rupture	4	
Strands embedded in ducts filled with grout	G-D3-S48-M (1)	168	227	242	19.3	Bond failure	1	Straight
	G-D3-S48-M (2)	203	230	275	40.6 (20.3)	Strand rupture	7 (3.5/strand)	
	G-D3-S48-M (I)	142	No wire was fractured	230	20	Bond failure	0	
	G-D3-S48-Cyclic	191 (second cycle to 200 ksi)	248	265	21	Strand rupture	4	
	G-D3-Curved60-M	No free-end slip was observed	230	268	19.5	Strand rupture	4	Curved

Note: (1) = one strand per duct; (2) = two strands per duct; 90Deg42 = 90-degree bent strand with free end and 42 in. embedment length; 90Deg54 = 90-degree bent strand with free end and 54 in. embedment length; Bulb0 = straight strand with bond-head anchorage and 0 in. embedment length; Bulb18 = straight strand with bond-head anchorage and 18 in. embedment length; Bulb22 = straight strand with bond-head anchorage and 22 in. embedment length; C = strand embedded in concrete; Cyclic = cyclic loading; Curved60 = curved strand with 60 in. embedment length; D3 = strand diameter of 0.3.75 in; D5 = strand diameter of 0.5 in.; D6 = strand diameter of 0.6 in.; G = strand embedded in grouted ducts; (I) = strand with initial stress; M = monotonic loading; n/a = not applicable; Plate18 = straight strand with end-plate anchorage and 18 in. embedment length; Plate24 = straight strand with end-plate anchorage and 24 in. embedment length; Plate30 = straight strand with end-plate anchorage and 30 in. embedment length; S48 = straight strand with free end and 48 in. embedment length; S54 = straight strand with free end and 54 in. embedment length. 1 in. = 25.4 mm; 1 kip = 4.448 N.; 1 ksi = 6.895 MPa.

ably, with the failure controlled by the rupture of both strands, which did not seem to cause the bond between the strands and surrounding grout to deteriorate as expected. However, both strands started to experience free-end displacement when the stress reached 203 ksi (1340 MPa) and the free-end displacement reached 0.07 in. (1.8 mm) at the end of the test, which was considerably smaller than the single strand subjected to cyclic loading. Applying an initial stress was detrimental to the bond capacity of the unstressed, grouted strands, which caused pullout failure. The loaded-end displacement increased significantly after the stress reached 150 ksi (1034 MPa) for the strand with an initial stress. The curved strand, which was used to simulate installation of a precast concrete girder in line with a column and with ducts placed around the column, performed satisfactorily. This observation implies that the curved duct configuration provided sufficient anchorage and the 0.375 in. (9.5 mm) diameter strand was fully developed within the 60 in. (1524 mm) ($160d_s$ where d_s is the strand diameter) curved embedment length.

Strain distribution Because the ultimate strand strength was not reached for the single strand in a duct when subjected to monotonic loading, the strain distribution along the embedment length was examined based on the data obtained from the pullout test conducted on the two strands in a duct and subjected to monotonic loading. Four strain gauges were placed along the embedment length with 12 in. (304.8 mm) spacing. **Figure 6** presents the measured strain distribution at stress levels ranging from 25 to 225 ksi (172 to 1551 MPa) and shows that the strain penetrated 24 and 36 in. (609.6 and 914.4 mm) embedment lengths when the strand stress reached 125 and 175 ksi (862 and 1207 MPa), respectively. At different stress levels, the strain distributions along the embedment length were almost parallel to each other. Therefore, it is reasonable to assume a constant bond stress between the strand and surrounding grout within the embedment length, which is estimated to be 472 psi (3.3 MPa) with a grout compressive strength of 4626 psi (31.9 MPa). This

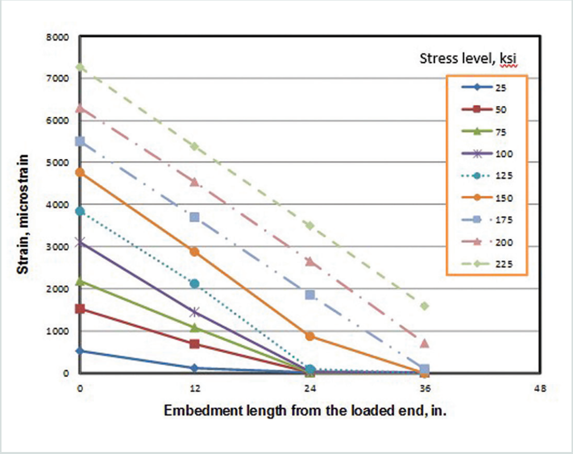

Figure 6. Measured strain distribution along the embedment length for two strands per duct subjected to monotonic loading at different stress levels. Note: 1 in. = 25.4 mm; 1 ksi = 6.895 MPa.

corresponds to a ratio of seven between the bond stress and the square root of the grout compressive strength. From this estimation, it was found that a 54 in. (1371.6 mm) ($144d_s$) embedment length was required to fully develop the strand up to its tensile strength (that is, 270 ksi [1862 MPa]). This finding is consistent with that reported by Adachi and Nishiyama[9] that the maximum average bond strength between a seven-wire strand and grout is about 435 psi (3 MPa).

Strands embedded in concrete

General behavior and failure modes For the strands embedded in concrete, the straight strands with bond-head and end-plate anchorage had a significantly reduced embedment length compared with the straight strands with free ends that were anchored along the entire length of the concrete block. The embedment length for the straight strands anchored with a 90-degree bend was reduced compared with the straight strands with free ends, but not as significantly as the strands with bond-head and end-plate anchorage details. The strands with an end-plate anchorage and a 90-degree bend experienced strand rupture failure, whereas the strands with bond-head anchorage experienced pullout failure. For the straight strands with free ends embedded with the same embedment length, the failure depended on the strand diameter and loading type. The 0.375 in. (9.5 mm) diameter straight strand experienced rupture failure when subjected to monotonic loading but pullout failure under cyclic loading. By contrast, the 0.6 in. (15.2 mm) diameter straight strand experienced pullout failure for both monotonic and cyclic loading. For the strands that experienced rupture failure, the maximum strand stress was approximately 270 ksi (1862 MPa).

Comparison of strand stress and loaded-end displacement **Figure 7** compares the relationship between the strand stress and loaded-end displacement for strands anchored in concrete with different anchorage details. The 0.375 in. (9.5 mm) diameter straight strands with free ends were embedded along the entire length of the concrete block (that is, the embedment length was 54 in. [1371.6 mm] [$144d_s$]) and subjected to monotonic and cyclic loading, respectively. During the test, the 0.375 in. diameter strand did not experience any obvious displacement at the free end when subjected to monotonic loading but started to experience free-end displacement when the stress reached 140 ksi (965 MPa) for cyclic loading. Therefore, a 54 in. straight embedment length was sufficient for the 0.375 in. diameter strand to develop its tensile strength subjected to monotonic loading; however, the strand with the same anchorage length experienced significant free-end displacement under cyclic loading. This is believed to be due to cyclic loading gradually deteriorating the bond between the strand and surrounding concrete. Therefore, the tension force was transferred to the surrounding concrete through the entire embedment length, resulting in an ultimate free-end displacement of 0.27 in. (6.9 mm) for cyclic loading.

For the 90-degree bent anchorage, the 0.375 in. (9.5 mm) diameter strands had a total embedment length of 42 in.

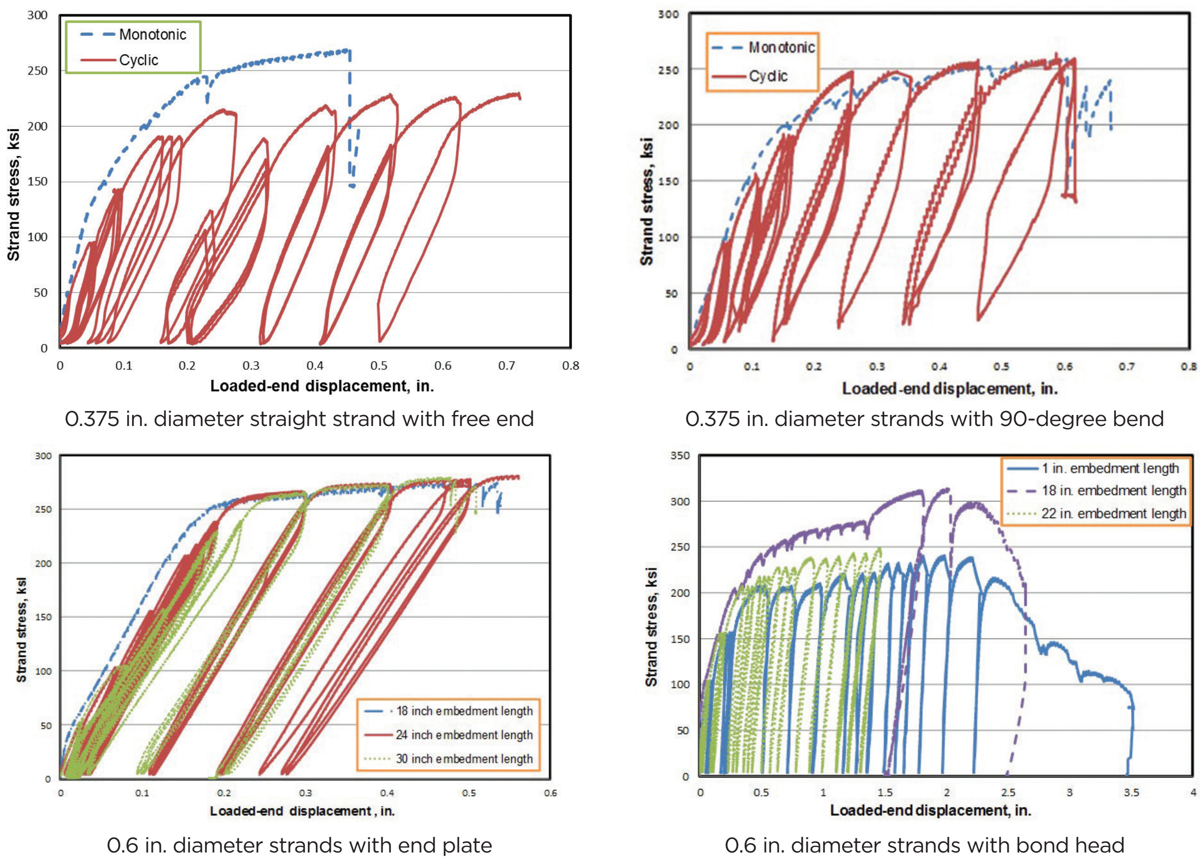

Figure 7. Strand stress–displacement response comparisons of strands anchored in concrete. Note: 1 in. = 25.4 mm; 1 ksi = 6.895 MPa.

(1066.8 mm) ($112d_s$), including a 6 in. (152.4 mm) ($16d_s$) pre-bent length, while the 0.5 in. (12.7 mm) diameter strands had a total embedment length of 56 in. (1422.4 mm) ($112d_s$), including an 8 in. (203.2 mm) ($16d_s$) pre-bent length. The strands were tested under both monotonic and cyclic loading. Figure 7 shows the strand stress versus loaded-end displacement responses of the 0.375 in. diameter strands. Based on this figure, the embedment length ($112d_s$) and pre-bent length ($16d_s$) designed for the strands tested in this study were sufficient to withstand both monotonic and cyclic loading. A similar response was obtained for the 0.5 in. diameter strands.

The performance of the straight strands anchored with an end plate was excellent. Figure 7 compares the responses of these strands with different embedment lengths. All strands with end-plate anchorage failed due to the rupture of strand wires and the embedment length did not considerably affect the ultimate capacity of the strands; however, the embedment length influenced the initial stiffness of the strand response. This indicates that the end-plate details can provide sufficient anchorage with significantly reduced embedment length, suggesting that most of the tension force is transferred through the plate instead of through the bond between the strands and surrounding concrete; however, the initial stiffness difference is attributed to the strain penetration that occurred along the embedment length. With the increase in the embedment length, more strain penetration occurred, which resulted in greater displacement at the loading end. This will be further examined in the next section.

Compared with the performance of strands with end-plate anchorage, the behavior of strands anchored with a bond head was poor. Two of these strands were tested without any significant embedment length and were subjected to both monotonic and cyclic loading. Figure 7 shows the measured strand stress and loaded-end displacement relationships of strands anchored in concrete with bond head for different embedment lengths. All strands experienced significant displacement at the loading end, followed by pullout failure. For the same embedment length of 18 in. (457.2 mm) ($30d_s$), it was found that the strands behaved very differently during the test. Therefore, the bond-head detail cannot provide dependable anchorage. The capacity can highly depend on how well the wires at the bond-head location bond to the surrounding concrete.

Influence of anchorage type **Figure 8** compares the envelope response of strand stress with loaded-end displacement responses for the 0.375 and 0.6 in. (9.5 and 15.2 mm)

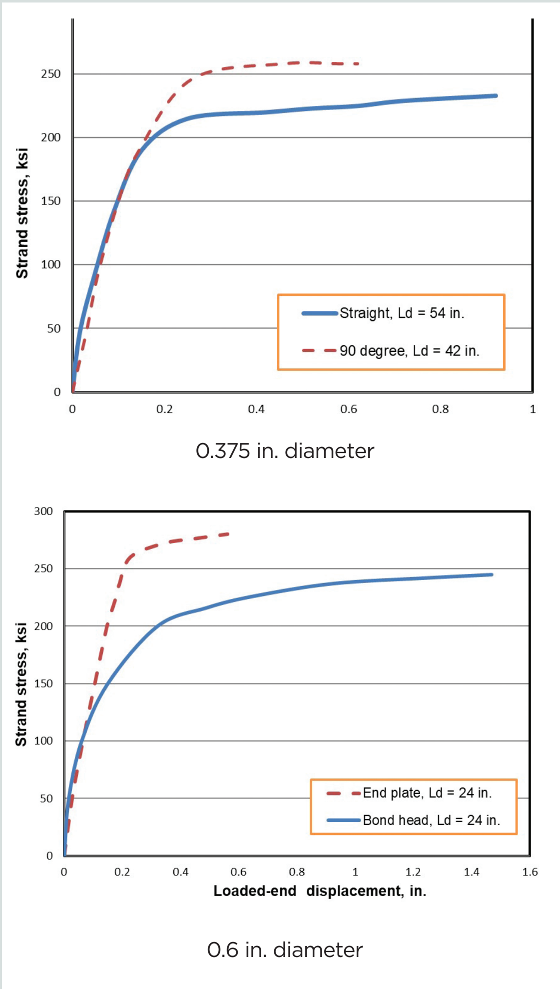

Figure 8. Influence of anchorage type on the strand stress and loaded-end displacement envelope response of strands anchored in concrete Note: L_d = embedment length; 1 in. = 25.4 mm; 1 ksi = 6.895 MPa.

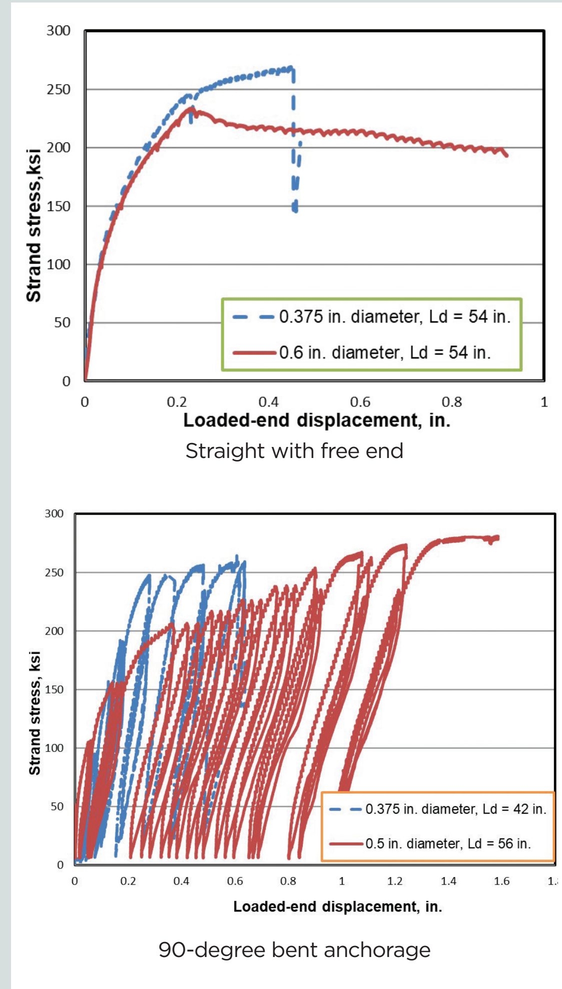

Figure 9. Influence of strand diameter on the strand stress and loaded-end displacement response of strands anchored in concrete. Note: L_d = embedment length; 1 in. = 25.4 mm; 1 ksi = 6.895 MPa.

diameter strands anchored in concrete with different anchorage types. Compared with the straight strand with free end, the strand with 90-degree bend reduces the embedment length while providing better performance. For the 0.6 in. diameter strands with 24 in. (609.6 mm) ($40d_s$) embedment length, the strand anchored with the end plate behaves considerably better than the bond-head anchorage, which experiences a significantly shorter elongation at the interface between the strand and the concrete block (0.6 in. compared with 1.5 in. [38.1 mm]) and also reaches a much higher capacity (270 ksi [1862 MPa] compared with 248 ksi [1710 MPa]).

Influence of strand diameter Figure 9 presents the results for straight strands with free ends and straight strands with a 90-degree bend. As shown, a 54 in. (1371.6 mm) ($90d_s$) straight embedment length was not sufficient for the 0.6 in. (15.2 mm) diameter strand to be fully developed when subjected to monotonic loading. When the strand stress reached 230 ksi (1586 MPa) ($0.85f_{pu}$), the loaded-end displacement continued to increase, along with gradually decreasing strand stress. This indicated that the strand stress was completely transferred to the free end of the strand as the strand stress reached 230 ksi for the 0.6 in. diameter straight strand. In addition, although the 0.5 in. (12.7 mm) diameter strand that was anchored with a 90-degree bend failed by strand rupture, it experienced significantly greater loaded-end displacement compared with the 0.375 in. (9.5 mm) diameter strand (1.6 in. [40.6 mm] compared with 0.6 in.), especially after the strand stress reached 200 ksi (1379 MPa) ($0.74 f_{pu}$).

Strain distribution Figure 10 presents the measured strain distribution along the embedment length for the strands anchored in concrete at different stress levels. The strain at a 52 or 39 in. (1320.8 or 990.6 mm) embedment length from the loaded end represents the strain measured at the center of the pre-bent length for the 0.5 and 0.375 in. (12.7 and 9.5 mm) diameter strands. The strain measured at the pre-bent length for the 0.5 in. diameter strand was approximately zero during the entire loading process, whereas the strain measured at the pre-bent length for the 0.375 in. diameter strand started to

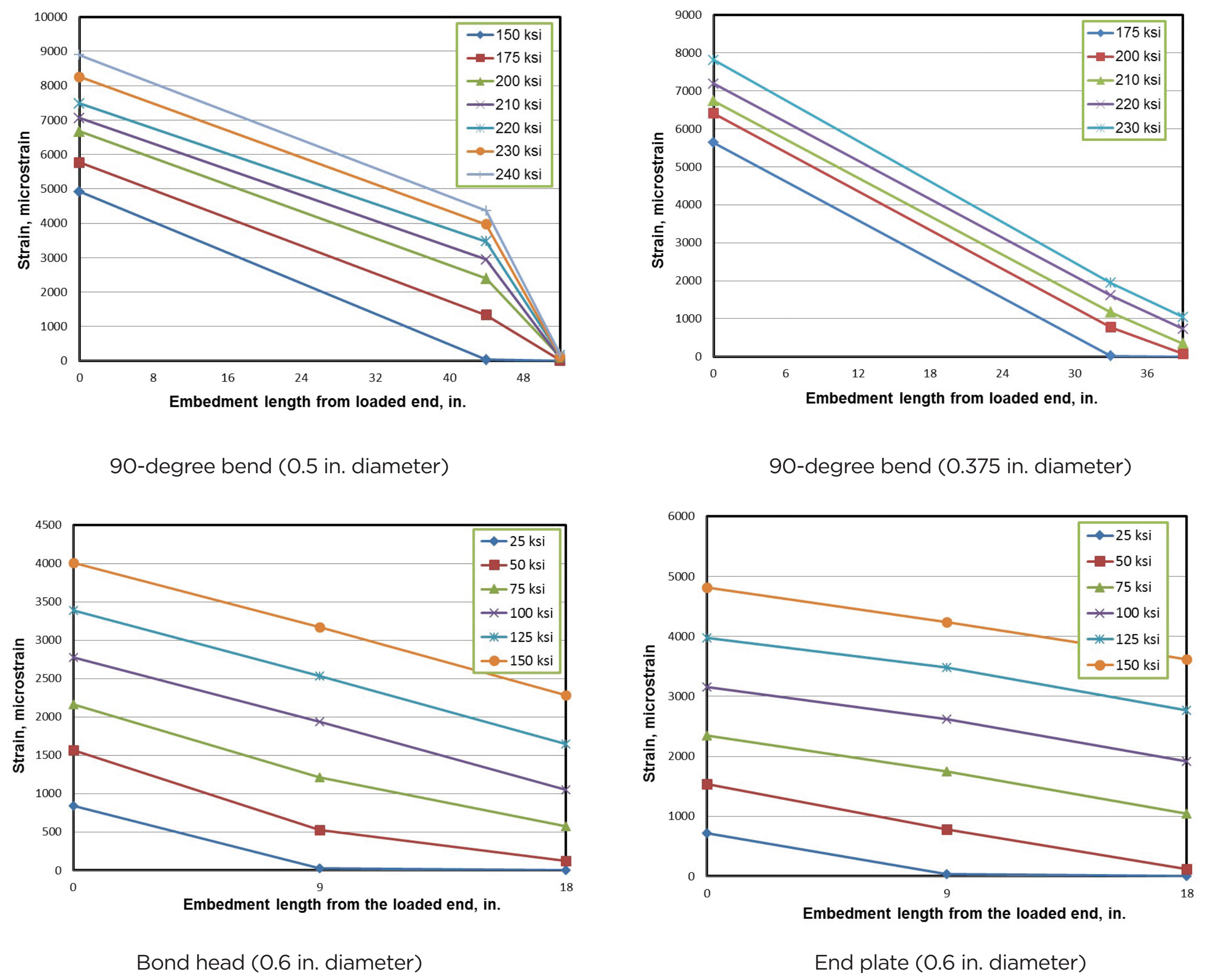

Figure 10. Measured strain distribution along the embedment length for strands anchored in concrete at different stress levels. Note: 1 in. = 25.4 mm; 1 ksi = 6.895 MPa.

increase when the strand stress reached 200 ksi (1379 MPa). This observation indicates that the 0.375 in. diameter strand experienced local slip at the bend location. Based on the measured strain distribution (Fig. 10), the strain penetrated to a 44 in. (1117.6 mm) embedment length for the 0.5 in. diameter strand when the strand stress reached 150 ksi (1034 MPa), whereas the strain penetrated to a 33 in. (838.2 mm) embedment length for the 0.375 in. diameter strand when the strand stress reached 175 ksi (1207 MPa). Figure 10 shows the measured strain distribution along the 18 in. (457.2 mm) embedment length for the 0.6 in. (15.2 mm) diameter strand anchored with a bond head and end plate, respectively. For both strands, the strain penetrated to a 9 in. (228.6 mm) embedment length when the strand stress reached 25 ksi (172 MPa). At the anchorage location, which was an 18 in. embedment length from the loaded end, both strands experienced large strains. Therefore, the force transferred at this location was primarily taken by the anchorage details. Similar to the strand embedded in grouted ducts, the strain distributions at each stress level were also almost parallel to each other. Therefore, it is reasonable to assume constant bond stress between the strand and surrounding concrete within the embedment length in this study.

Anchorage capacity for strands embedded in concrete

Based on the strains measured at the anchorage location, the force transferred through the anchorage F_a can be calculated as shown in Eq. (1) and the force transferred through the bond F_b can then be calculated by subtracting the force taken by the anchorage from the total applied force (Eq. [2]).

$$F_a = \varepsilon_a E_s A_s \tag{1}$$

where

ε_a = measured strand strain at the anchorage location

E_s = nominal modulus of elasticity of strand

A_s = nominal cross-sectional area of strand

$$F_b = F_t - F_a \tag{2}$$

where

F_t = total applied force

Before the strain penetrated to the anchorage location, almost all of the force was transferred through the bond between the strand and surrounding concrete. **Figure 11** presents the percentage of the total force that was transferred through either bond or anchorage as a function of strand stress. According to this figure, the force was primarily transferred through bond for the strands anchored with a 90-degree bend (that is, 100% at strand stress of 150 ksi [1034 MPa] and 90% and 65% at strand stress of 200 ksi [1379 MPa] for 0.375 in. [9.5 mm] and 0.5 in. [12.7 mm] diameter strands, respectively), and mainly transferred through anchorage for the strands anchored with an end plate (that is, 70% at strand stress of 150 ksi).

Analytical program

The analytical model in this study was based on a one-dimensional finite element analysis. The strand within the embedment length was divided into a discrete number of small elements. Based on the experimental measured strain distribution for strands anchored in grout or concrete with different anchorage types, linear strain distribution along the embedment length was assumed. The strand stress, local slip, and bond stress variations along the embedment length could therefore be calculated based on the force equilibrium and compatibility conditions.

The analytical model incorporates three basic elements: a typical stress-strain relationship for the strand, a linear strain distribution along the embedment length, and force equilibriums and compatibility conditions.

The analytical model assumed that the anchorage was sufficient to fully develop the strand studied in this paper, which means that the local slip at the anchorage location was assumed to be zero; however, based on the measured strain distribution for the 0.375 in. (9.5 mm) diameter strand anchored in concrete with a 90-degree bend (top right graph in Figure 10), the strains penetrated to the pre-bent length. Therefore, the embedment length for this strand was considered to be the entire embedment length of 42 in. (1066.8 mm) in the analytical study, rather than 36 in. (914.4 mm).

Figure 12 shows the comparison between the assumed and measured strain distribution along the embedment length at different stress levels. Based on this assumed strain distribution, the derived analytical strand stress and loaded-end displacement relationship for the strands anchored in concrete with different anchorage types was compared with the experimental measured response (**Fig. 13**). Figure 13 shows that the analytical model used in this study represented the measured responses fairly accurately, except for the strand anchored with a bond head. The analytical loaded-end displacement is significantly smaller than the measured one. The difference starts to occur as the strand stress reaches 100 ksi (689.5 MPa), and it becomes greater as the strand stress continues to increase. This difference was believed to come from the local slip at the bond-head location, which was confirmed by the experimental data.

As previously discussed, the experimental measured strain distribution confirmed a linear strain distribution along the embedment length. Therefore, the bond stress was uniformly

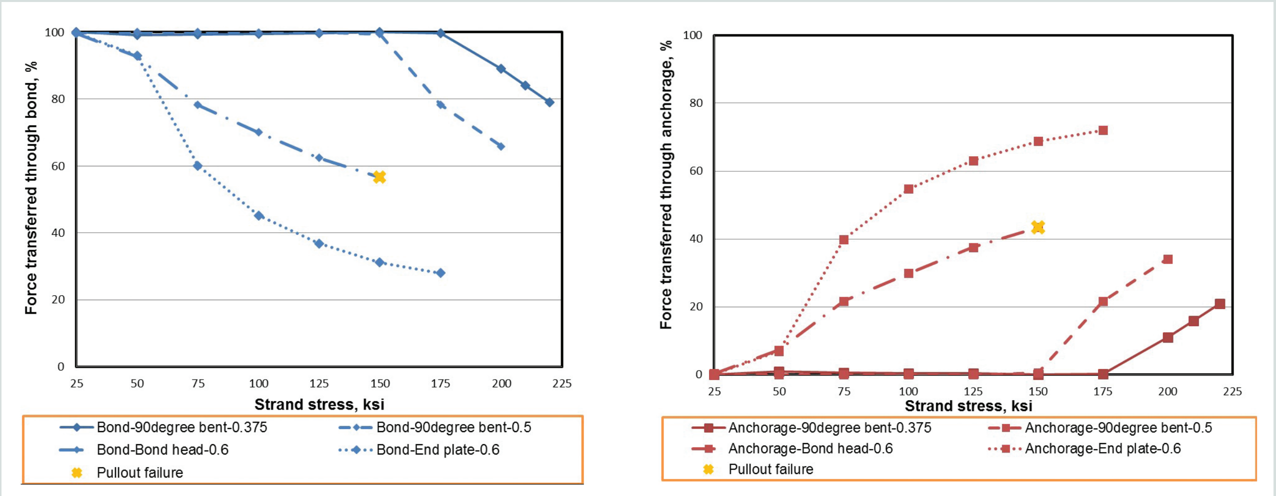

Figure 11. Percentage of total applied force transferred through bond and anchorage for different anchorage types and strand diameters. Note: 1 in. = 25.4 mm; 1 ksi = 6.895 Mpa.

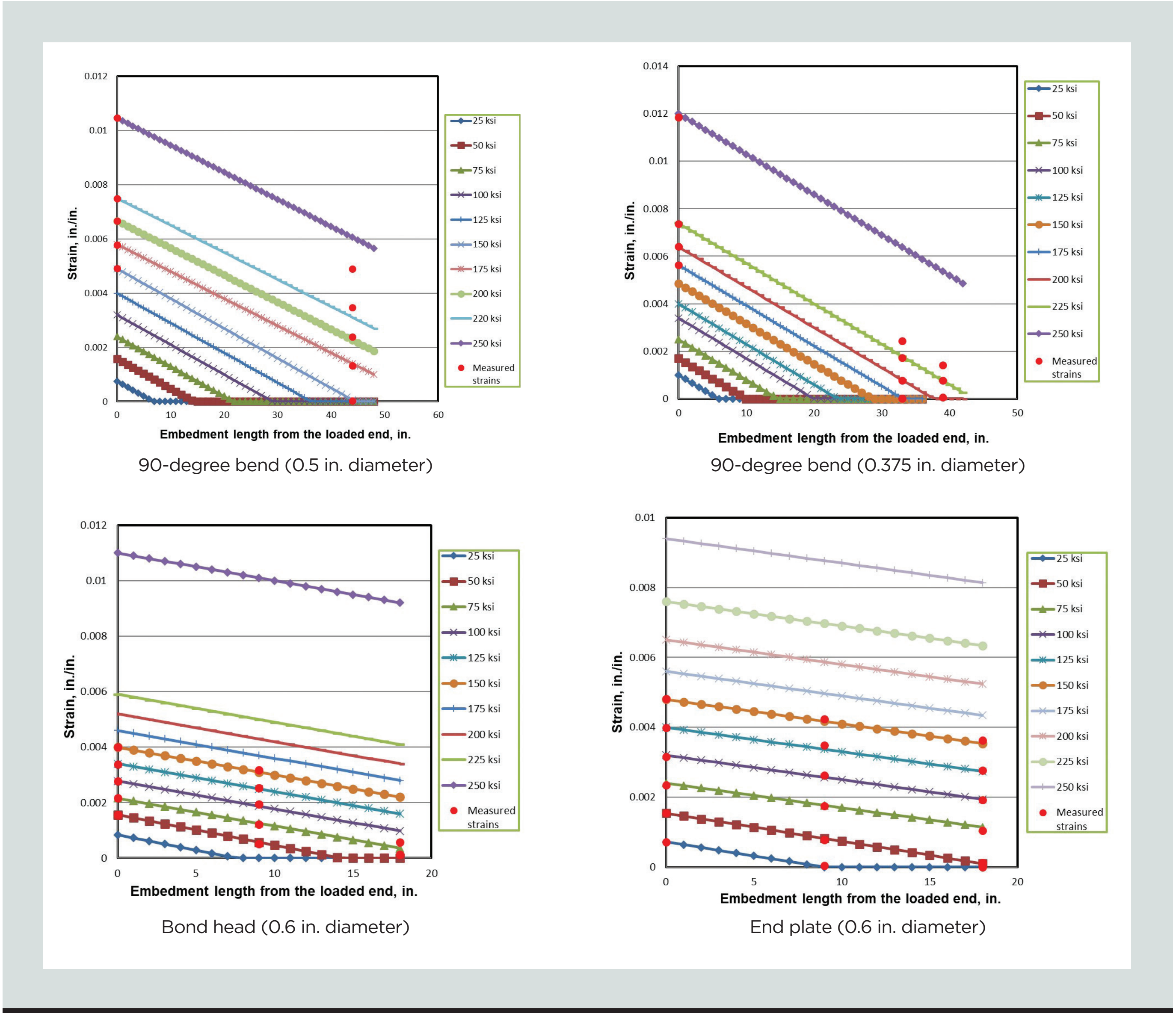

Figure 12. Measured and analytical strain distribution comparisons for strands anchored in concrete at different stress levels. Note: 1 in. = 25.4 mm; 1 ksi = 6.895 MPa.

distributed along the portion of the embedment length before and after the strand yielded, then

$$F_b = \pi d_s L_b \tau$$

where

L_b = bonded length of strand

τ = bond stress

To account for the effect of concrete compressive strength, the bond stress was normalized to a typical concrete compressive strength of 4500 psi (31 MPa). **Table 3** shows the back calculated bond stress values from the analytical study in this research and the research conducted by Salmons and McCrate[3] before the strand yielded. After the strand yielded, the bond stress reduced significantly. The ratio between the bond stress and the square root of concrete compressive strength n was calculated and the average n was 5.8 for monotonic loading and 4.3 for cyclic loading. Therefore, the bond stress between the unstressed strand and surrounding concrete is recommended to be five times the square root of the concrete compressive strength.

Conclusion

The experimental and analytical study conducted in this research focused on unstressed strands as connection reinforcement between precast concrete girders and cap beams for seismic applications and provided qualitative and quantitative measurements to evaluate the load-transfer characteristics of unstressed strands anchored in grout and concrete with different anchorage types. Although the experimental study was designed based on precast concrete bridge girder applications, the suggested embedment length and average bond stress of unstressed strands anchored in grout and concrete can also be applied to other scenarios involving connections of precast concrete members using

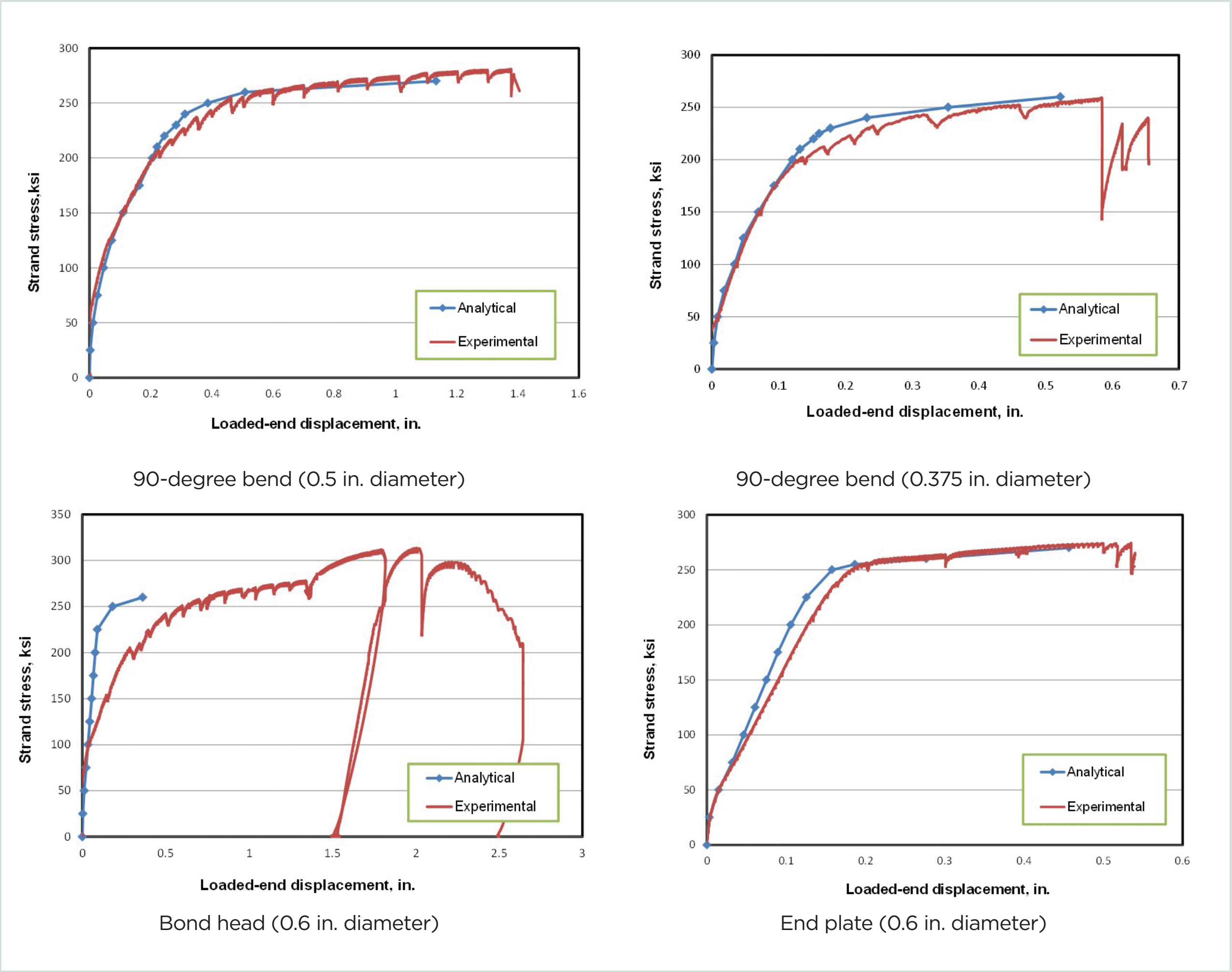

Figure 12. Measured and analytical strain distribution comparisons for strands anchored in concrete at different stress levels. Note: 1 in. = 25.4 mm; 1 ksi = 6.895 MPa.

unstressed strands. A summary of findings and recommendations is offered:

- For strands embedded in grouted ducts, applying initial stress was detrimental to the bond capacity between the strand and surrounding grout.

- Placing two strands per duct did not seem to deteriorate the bond capacity between the strand and surrounding grout. A bonded length of 54 in. (1371.6 mm) ($144d_s$) was sufficient to transfer the force for straight strands embedded in grouted ducts up to the wire rupture.

- Tendon curvature was beneficial to fully develop the strand embedded in grouted ducts and concrete.

- For strands embedded in concrete, the end-plate anchorage provided the best performance of the four anchorage details if the strand chucks, which included bearing plates, barrel anchors, and wedges, were assembled correctly.

- The end-plate anchorage reduced the bonded length of strand significantly while maintaining satisfactory behavior. There were no noticeable differences in the behavior of strands with this type of anchorage with various bonded lengths (18 in. [457.2 mm] [$30d_s$], 24 in. [609.6 mm] [$40d_s$], and 30 in. [762 mm] [$50d_s$]). The measured strain data validated that the applied force was primarily taken by the plate once the strain penetrated to the anchorage location and 18 in. bonded length was adequate to fully develop the strand with end-plate anchorage.

- The performance of the bond-head anchorage was not reliable. It can highly depend on how well the plastically deformed wires bond to the surrounding concrete. The strand anchored with a bond head experienced significant loaded-end displacement without fracturing the strand. Furthermore, the local slip at the bond-head location started to occur as the strand stress reached 100 ksi (689.5 MPa) ($0.37f_{pu}$).

- An embedment length of $112d_s$ with a pre-bent length

Table 3. Back calculated bond stress values between unstressed strand and surrounding concrete

Researchers	d_s, in.	f'_c, psi	Anchorage	L_d, in.	Loading type	τ, psi	$\tau' = \tau\frac{\sqrt{4500}}{f'_c}$, psi	$n = \frac{\tau'}{\sqrt{4500}}$
Liang and Sritharan	0.375	4000	Straight	54 ($144d_s$)	Monotonic	450	477	7.1
	0.375	4000		54 ($144d_s$)	Cyclic	206	218	3.3
	0.6	4000		54 ($90d_s$)	Monotonic	490	520	7.7
	0.375	4000	90-degree bent	42 ($112d_s$)	Monotonic	350	371	5.5
	0.375	4000		42 ($112d_s$)	Cyclic	350	371	5.5
	0.5	3850		56 ($112d_s$)	Monotonic	305	330	4.9
	0.5	3850		56 ($112d_s$)	Cyclic	305	330	4.9
	0.6	4000	Bond head	18 ($30d_s$)	Monotonic	328	348	5.2
	0.6	3850		22 ($37d_s$)	Cyclic	230	249	3.7
	0.6	3850	End plate	24 ($40d_s$)	Monotonic	262	283	4.2
	0.6	3850		30 ($50d_s$)	Cyclic	262	283	4.2
	Average/standard deviation							5.8/1.35 (monotonic), 4.3/0.9 (cyclic)
Salmons and McCrate (1977)	0.5	6320	Straight	45 ($90d_s$)	n/a	275	232	3.5
	0.5	5660		30 ($60d_s$)	n/a	310	276	4.1
	0.5	6610		20 ($40d_s$)	n/a	360	297	4.4
	0.5	7090	90-degree bent	40 ($80d_s$)	n/a	486	387	5.8
	0.5	7150		30 ($60d_s$)	n/a	555	440	6.6
	0.5	6340		20 ($40d_s$)	n/a	430	262	5.4
	Average/standard deviation							5/1.15

Note: d_s = strand diameter; f'_c = concrete compressive strength; L_d = embedment length; n/a = not applicable; τ = bond stress; τ' = bond stress normalized to 4500 psi of concrete compressive strength. 1 in. = 25.4 mm; 1 psi = 6.895 kPa.

of $16d_s$ was sufficient for unstressed bent strands to be fully developed when subjected to both monotonic and cyclic loading.

- Based on the measured strain data in the experimental study, a linear strain distribution along the embedment length for strand anchored in both grout and concrete was assumed. The analytical relationship between the strand stress and displacement at the loading end corresponded well to the measured response, which confirmed the linear strain distribution assumption.

- The average bond stress normalized to 4500 psi (31 MPa) of concrete compressive strength was 335 psi (2.3 MPa), which resulted in a ratio of five between the bond stress and the square root of concrete compressive strength. Similarly, for the strands embedded in grouted ducts, the average bond stress normalized to 4500 psi of grout compressive strength was 466 psi (3.2 MPa), which resulted in a ratio of seven between the bond stress and the square root of grout compressive strength.

Acknowledgments

The authors would like to acknowledge the financial support from the California Department of Transportation, the National Natural Science Foundation of China under grant 51808380, and the Tianjin Municipal Science and Technology Commission under grant 17JCYBJC42500.

References

1. Stevens, G., and J. Harris. 2006. "Chapter 7: Precast Concrete Design." In NEHRP Recommended Provisions: Design Examples, FEMA 451, pp. 7-1 to 7-66. Washington, DC: Federal Emergency Management Agency.

2. AASHTO (American Association of State Highway and

Transportation Officials). 2012. *AASHTO LRFD Bridge Design Specifications*. 6th ed., customary U.S. units. Washington, DC: AASHTO.

3. Salmons, J., and T. McCrate. 1977. "Bond Characteristics of Untensioned Prestressing Strand." *PCI Journal* 22 (1): 52–65.

4. Noppakunwijai, P., N. Jongpitakseel, Z. Ma, S. A. Yehia, and M. K. Tadros. 2002. "Pullout Capacity of Non-Prestressed Bent Strands for Prestressed Concrete Girders." *PCI Journal* 47 (4): 90–103.

5. Miller, R., R. Castrodale, A. Mirmiran, and M. Hastak. 2004. "Connection of Simple-Span Precast Concrete Girders for Continuity." Washington, DC: The National Academies Press. https://doi.org/10.17226/13746.

6. Caltrans (California Department of Transportation). 2013. *Seismic Design Criteria*. Version 2.0. Sacramento, CA: Caltrans.

7. Vander Werff, J., R. Peggar, Z. Cheng, and S. Sritharan. 2015. "Seismic Performance of Girder-to-Cap Connections for Accelerated Bridge Construction of Integral Bridges." Report CA16-2265. Sacramento, CA: Caltrans.

8. Vander Werff, J., R. Snyder, S. Sritharan, and J. Holombo. 2015. "A Cost-Effective Integral Bridge System with Precast Concrete I-Girders for Seismic Application." *PCI Journal* 60 (5): 76–95.

9. Adachi, M., and M. Nishiyama. 2000. "Idealization of Hysteretic Behavior of Prestressed Concrete Members and Assemblages Considering Bond-Slip between Prestressing Steel and Concrete." In *12th World Conference on Earthquake Engineering: Proceedings, January 30 to February 4, 2000, Auckland, New Zealand*. Paper 2259. Wellington, NZ: New Zealand Society for Earthquake Engineering.

Notation

a = pre-bent length

A_s = nominal cross-sectional area of strand

d_s = nominal diameter of strand

E_s = nominal modulus of elasticity of strand

f_c' = concrete compressive strength

f_{py} = yield strength of prestressing steel

f_{pu} = specified tensile strength of prestressing steel

f_s = strand stress

F = applied force

F_a = force transferred through the anchorage

F_b = force transferred through the bond

F_t = total applied force

L_b = bonded length of strand or embedment length

L_d = embedment length

n = ratio between the bond stress and square root of concrete compressive strength

ε_a = measured strand at the anchorage location

τ = bond stress

τ' = bond stress normalized to 4500 psi of concrete compressive strength

About the authors

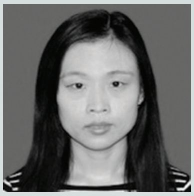

Xiao Liang, PhD, is a lecturer in the School of Civil Engineering at Tianjin Chengjian University in Tianjin, China.

Sri Sritharan, PhD, is a professor in the Department of Civil, Construction and Environmental Engineering at Iowa State University in Ames, Iowa.

Abstract

Precast concrete members need to be connected effectively to form an integral structural system. Use of unstressed strands provides a cost-effective and practical solution to reinforce the connection regions of precast concrete members, especially for precast concrete bridge girder applications. With the limited understanding of bonding characteristics for unstressed strands, a combination of experimental and analytical programs, which focused on unstressed strands as a connection between precast concrete girders and cap beams for seismic applications, was designed to investigate the fundamental load-transfer characteristics of unstressed strands anchored in grout and concrete based on pullout tests. The relationship between strand stress and loaded-end displacement was developed, and the bond stress of unstressed strands embedded in concrete and grouted duct was examined. The average bond stress of unstressed strands anchored in concrete and grouted duct is recommended to be five and seven times the square root of concrete compressive strength, respectively. The results of this research provide qualitative embedment length requirements to design connections between precast concrete members using unstressed strands.

Keywords

Anchorage, bond stress, connection, strain distribution, unstressed strand, seismic.

Review policy

This paper was reviewed in accordance with the Precast/Prestressed Concrete Institute's peer-review process.

Reader comments

Please address any reader comments to PCI Journal editor-in-chief Tom Klemens at tklemens@pci.org or Precast/Prestressed Concrete Institute, c/o PCI Journal, 8770 W. Bryn Mawr Ave., Suite 1150, Chicago, IL 60631.